Acta Biomaterialia 7 (2011) 1653–1664

Contents lists available at ScienceDirect

Acta Biomaterialia

journal homepage: www.elsevier.com/locate/actabiomat

Fabrication of porous chitosan scaffolds for soft tissue engineering using dense gas CO_2

Chengdong Ji [a], Nasim Annabi [a], Ali Khademhosseini [b,c], Fariba Dehghani [a,*]

[a] School of Chemical and Biomolecular Engineering, University of Sydney, Sydney, Australia
[b] Harvard-MIT Division of Health Sciences and Technology, Massachusetts Institute of Technology, Cambridge, MA 02139, USA
[c] Center for Biomedical Engineering, Department of Medicine, Brigham and Women's Hospital, Harvard Medical School, Boston, MA 02115, USA

ARTICLE INFO

Article history:
Received 2 August 2010
Received in revised form 25 November 2010
Accepted 30 November 2010
Available online 3 December 2010

Keywords:
Chitosan hydrogel
Porosity
Glutaraldehyde
Genipin
Dense gas CO_2

ABSTRACT

The aim of this study was to investigate the feasibility of fabricating porous crosslinked chitosan hydrogels in an aqueous phase using dense gas CO_2 as a foaming agent. Highly porous chitosan hydrogels were formed by using glutaraldehyde and genipin as crosslinkers. The method developed here eliminates the formation of a skin layer, and does not require the use of surfactants or other toxic reagents to generate porosity. The chitosan hydrogel scaffolds had an average pore diameter of 30–40 μm. The operating pressure had a negligible effect on the pore characteristics of chitosan hydrogels. Temperature, reaction period, type of biopolymer and crosslinker had a significant impact on the pore size and characteristics of the hydrogel produced by dense gas CO_2. Scanning electron microscopy and histological analysis confirmed that the resulting porous structures allowed fibroblasts seeded on these scaffolds to proliferate into the three-dimensional (3-D) structure of these chitosan hydrogels. Live/dead staining and MTS analysis demonstrated that fibroblast cells proliferated over 7 days. The fabricated hydrogels exhibited comparable mechanical strength and swelling ratio and are potentially useful for soft tissue engineering applications such as skin and cartilage regeneration.

1. Introduction

In vitro tissue constructs are prepared by seeding cells on a suitable scaffold such as a porous hydrogel. These tissue constructs may be subsequently implanted for medical applications [1]. Biocompatibility, biodegradability, mechanical properties and porosity are important parameters for selection of a desirable scaffold for tissue engineering applications [2]. A class of materials that has attracted a great deal of attention as tissue engineering scaffolds are polysaccharide-based hydrogels [3,4]. Chitosan is polysaccharide that degrades in the presence of naturally occurring enzymes such as lysozyme [5–7]. The low mechanical strength of chitosan hydrogel can be improved by using a crosslinker such as glutaraldehyde (GA) [8,9], genipin (GP) [10], 1-ethyl-3(3-dimethylaminopropyl) carbodiimide hydrochloride (EDC) [11] or tripolyphosphate [12].

Solvent casting/salt leaching [13], freeze-drying [14,15] and gas foaming [16] have been used to generate porosity in chitosan and composite mixtures of chitosan and other polymers. The disadvantages of these techniques include the use of toxic solvents, the removal of solvent by evaporation (which takes days or even weeks), labour-intensive processing, irregularly shaped pores, insufficient interconnectivity and the inability to culture cells throughout the hydrogel scaffold [17]. Thus, it is desirable to develop methods to generate 3-D chitosan scaffolds on which cells can be cultured both on the surface of interconnected pores and within the bulk hydrogel.

Dense gas foaming is a technique to create pores in polymeric matrices by rapid gas expansion. Dense gases are fluids that are near or above their critical point, generally with a reduced temperature (T/T_c), and pressure (P/P_c) of 0.9–1.2. Carbon dioxide (CO_2) is the most commonly used dense gas because of its moderate critical properties (P_c = 73 bar and T_c = 31 °C), low toxicity and non-flammability [18]. A number of dense gas-related techniques have been developed to generate porosity for tissue engineering applications. For example, gas foaming by dense gas decompression is a rapid and commonly used process for forming uniform pores in polymers such as poly(lactic acid) (PLA) [19,20] and poly(lactic-co-glycolic acid) (PLGA) [21–23] without solvent. However, the dense gas technique is not efficient in creating pores in hydrophilic and glassy polymers such as chitosan because of the low solubility of CO_2 in these compounds. To overcome this problem, a co-solvent such as ethanol or diluted acid was previously used to improve the dissolution of a dense gas into the aqueous solution to produce porous hydrogels. However, only closed-pores were produced by using this method, and an extra heating step was needed to form open pores [24].

* Corresponding author.
E-mail address: fariba.dehghani@sydney.edu.au (F. Dehghani).

1742-7061/$ - see front matter © 2010 Published by Elsevier Ltd. on behalf of Acta Materialia Inc.
doi:10.1016/j.actbio.2010.11.043

A CO_2–water emulsion-templated system was also developed to produce highly porous structures in hydrophilic polymers such as alginate [25], poly(vinyl alcohol) (PVA) and chitosan [26,27]. In these systems, prefabricated surfactants such as PVAc-*b*-PEG-*b*-PVAc (M_w = 2000–2000–2000 g mol^{-1}) were used to generate a stable CO_2–surfactant–water emulsion. Open porous structures (~30 μm) were obtained due to the crosslinking and gelation of the aqueous phase in the polymers [26]. CO_2-assisted methods such as CO_2-induced phase inversion [28] and solvent exchange/supercritical fluid drying [29–31] were developed to produce porous hydrophilic polymers. However, these methods have limitations such as the use of organic solvents and the inability to form microscale pores that are suitable for tissue engineering.

Recently we have demonstrated the feasibility of creating pores in elastin, which is a hydrophilic polymer, by dissolving dense gas CO_2 at 60 bar and 37 °C in an aqueous phase prior to crosslinking the polymer [32]. By using this method, highly interconnected pores with an average pore diameter of 5 μm were formed; the thin-walled structures of these hydrogels allowed for rapid nutrient and oxygen transfer and fibroblast proliferation [32]. The mechanism of pore formation relies on dissolving CO_2 in the aqueous phase by pressurization of system and the formation of CO_2 gas bubbles in the polymer-rich phase during the depressurization. The objective of this study was to assess the feasibility of using this one-stage dense gas process to fabricate homogeneous polysaccharide-based hydrogels with larger pore diameters. Chitosan was crosslinked with either GA or GP in the presence of dense gas CO_2. The effects of process variables and crosslinker on the properties of chitosan hydrogels, including pore characteristics, swelling ratio, mechanical strength and cell proliferation, were examined and compared with those fabricated under atmospheric conditions.

2. Materials and methods

2.1. Materials

Chitosan (medium molecular weight), GA (25 vol.%), GP, Dulbecco's modified eagle medium (DMEM), fetal bovine serum (FBS), pen-strep, fluorescein diacetate (FDA), propidium iodide (PI) and hexamethyldislazane (HMDS) were purchased from Sigma. MTS ([3-(4,5-dimethylthiazol-2-yl)-5-(3-carboxymethoxyphenyl)-2-(4-sulfophenyl)-2H-tetrazolium) reagent was purchased from Promega. Tris($(HOCH_2)_3CNH_2$) was purchased from Merck. A 0.2 M acetic acid solution was prepared using glacial acetic acid (Ajax Fine Chem) in milliQ water. Phosphate-buffered saline (PBS) was prepared by dissolving PBS tablets (Sigma) in milliQ water. Food-grade CO_2 (99.99% purity) was supplied by BOC.

2.2. Hydrogel fabrication

2.2.1. Hydrogel fabrication under atmospheric conditions

A set of experiment was conducted prior to the dense gas CO_2 process to determine the required amount of crosslinker, time and temperature for chitosan hydrogel fabrication. In each experiment, chitosan was dissolved in 0.2 M acetic acid solution to prepare a 1.5 wt.% solution. High concentrations of chitosan were not used because of the high viscosity of the resulting solution and inadequate mixing, which resulted in the formation of a non-homogeneous hydrogel. Chitosan solutions were crosslinked at atmospheric conditions with GA at different temperatures, i.e. 4, 23 and 37 °C. Predetermined amounts of GA and chitosan solution were mixed to prepare different ratios. The mixtures were stirred for 1 min to make a homogeneous mixture and were kept at the desired temperatures for various durations. The effect of variables such as temperature, type of crosslinkers, ratio of crosslinker/chitosan and reaction time were investigated (Table 1). The optimized conditions were selected based on hydrogel formation status.

2.2.2. Hydrogel fabrication using dense gas CO_2

Prior to undertaking the dense gas CO_2 process for porosity generation in chitosan hydrogels, it is critical to obtain data for CO_2 solubility in the aqueous phase at different conditions. The data adopted from the literature in Fig. 1 demonstrate that at different temperatures (0–40 °C) the solubility of CO_2 in the water phase dramatically increases as the pressure is increased. CO_2 solubility is within 0.077 mol CO_2/kg H_2O at 1 bar and increases at least

Table 1
Optimization of chitosan crosslinking with different crosslinkers at different conditions under atmospheric conditions.

Crosslinkers	Temperature (°C)	Crosslinking ratio (%)	Crosslinking time				
			15 min	1 h	1.5 h	2 h	3 h
GA	4	0.125	–	–	–	–	–
		0.25	–	–	–	–	–
		0.5	–	–	+	+	+
	23	0.125	–	–	–	+	+
		0.25	–	–	+	+	+
		0.5	–	+	+	+	+
	37	0.125	–	+	+	+	+
		0.25	–	+	+	+	+
		0.5	–	+	+	+	+
GP	4	0.05	–	–	–	–	–
		0.125	–	–	–	–	–
		0.25	–	–	–	–	–
		0.5	–	–	–	–	–
	23	0.05	–	–	–	–	–
		0.125	–	–	–	–	–
		0.25	–	–	–	–	–
		0.5	–	–	–	–	–
	37	0.05	–	–	–	–	–
		0.125	–	–	–	–	–
		0.25	–	–	–	–	+
		0.5	–	–	–	–	+

1.5 wt.% chitosan solution was used.
Crosslinking ratio refers to the ratio of GA (v/v) or GP (w/v) in the whole mixture. +, Stable gel formation; –, unstable gel or no gel formation; circled areas refer to the conditions selected for high-pressure tests.

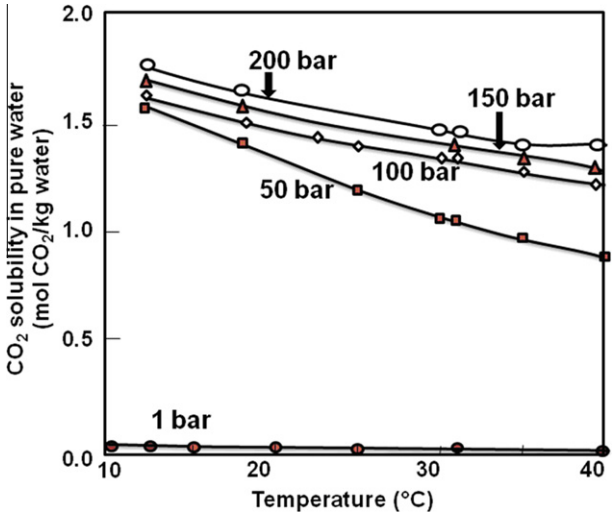

Fig. 1. Solubility of CO_2 in water as a function of variations in temperature and pressure [33].

30-fold at 50 bar. As expected, the solubility of CO_2 is decreased by increasing the temperature at each pressure [33]. The presence of salt and other compounds in the aqueous phase may affect the CO_2 solubility. However, the solubility data can be used as a basis to determine the operating conditions to enhance CO_2 solubility in the aqueous phase to create porosity in a hydrogel. The addition of CO_2 at high pressure (60 bar) to an aqueous solution can decrease the pH to 3 [34]. No significant effect was observed on crosslinking of hydrophilic polymers such as elastin by this pH drop [32].

The procedure for the preparation of hydrogels by dense gas CO_2 was described in detail in a previous study [32]. As shown in Fig. 2, in each experiment, a homogeneous mixture of chitosan solution and GA (below the toxic level (0.6 vol.%) [35]) was added to a custom-made high-pressure vessel (5 ml). After thermal equilibrium was established, the system was gradually pressurized with CO_2 using a high-pressure pump (ISCO Syringe pump, Model 500D) to a predetermined pressure between 60 and 160 bar (Fig. 2a); the pressure was maintained to allow for CO_2 saturation and chitosan crosslinking for a set period of time (Fig. 2b). The system was then depressurized at 10 bar min^{-1}, resulting in the generation of numerous gas bubbles which induce gas foaming (Fig. 2c). Faster depressurization rates were not used as these resulted in rapid venting and formation of non-homogeneous pores in the hydrogel matrix. The hydrogel was then collected and immersed in 0.1 M Tris in PBS for 1 h to inhibit further crosslinking. The immersed sample was finally rinsed three times with PBS and stored in PBS for at least 24 h to ensure the residual level of GA was below 5 ppm to minimize cytotoxicity [36].

Ginty et al. have demonstrated that mammalian cells can be encapsulated in a polymer matrix such as poly (DL-lactic acid) ($P_{DL}LA$) using a gas foaming technique [37]. However, the viability of cells was dramatically decreased after 5 min processing time [37]. It might be possible to incorporate cells during the pore formation step to minimize cell exposure to high-pressure CO_2 and decrease the amount of free crosslinker present in the system.

2.2.3. In vitro cell culture

To culture the cells on the fabricated chitosan hydrogels, a single fabricated hydrogel (~8 mm diameter) was transferred to a 24-well plate and washed with ethanol for sterilization. Previous studies have demonstrated that supercritical CO_2 has sterilization properties [38,39]. However, a standard sterilization procedure was performed in this study to minimize the number of factors that need to be considered for the in vitro study. After the ethanol wash step, the hydrogels were rinsed with culture media (DMEM, 10% FBS, 1% pen-strep) to remove residual ethanol and immersed in culture media at 37 °C overnight. The cells (human skin fibroblast cells GM3348) were then seeded onto the hydrogels at a concentration of 1×10^5 cells $sample^{-1}$ (for MTS assay, a cell concentration of 1×10^4 cells $sample^{-1}$ was used). The cell-seeded hydrogel were kept in a CO_2 (5% CO_2 and 95% humidity) incubator at 37 °C for further characterizations. The media was refreshed every 2 days.

2.3. Characterizations

2.3.1. Scanning electron microscopy analysis

The surface morphology of the chitosan was analyzed using scanning electron microscopy (SEM, Philips XL30). In this study, a cryo-SEM technique was used without any dehydration or coating treatment [40]. In brief, the fresh sample was mounted on a brass block. The block was then immersed in liquid nitrogen for 45 s, and immediately transferred into a vacuum chamber ($<1.3 \times 10^{-4}$ mbar) for viewing at 15 kV. The snap freezing of the hydrogel ensured that the images acquired represent a snapshot of the actual hydrogel structure as it exists under real hydration conditions [40]. The equivalent circle diameter (ECD) of the pores was calculated using Image J software. At least 300 pores were analyzed for each condition.

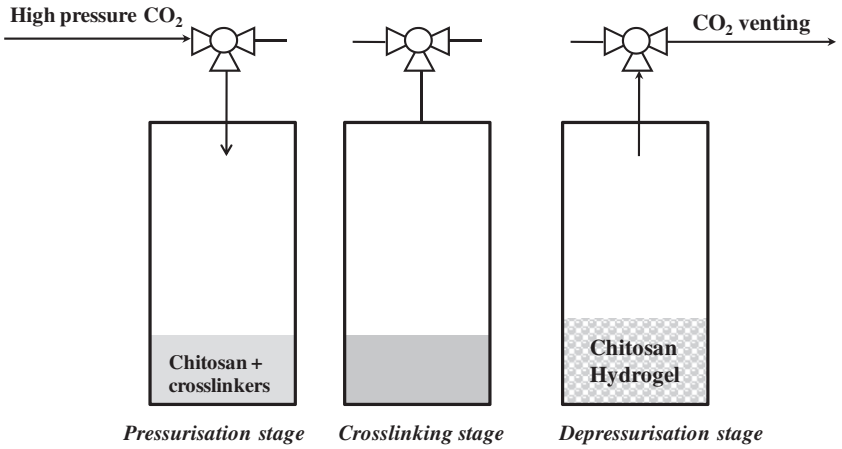

Fig. 2. Schematic diagram of the dense gas process during (a) the pressurization stage, (b) the crosslinking stage and (c) the depressurization stage.

For the cell-seeded samples, the hydrogels (4 day culture) were fixed with 2.5 vol.% GA solution in 0.1 M phosphate buffer for 1 h at 37 °C. To analyze the cross-section of cell-seeded hydrogels, they were cut with a razor blade before fixation. The fixed samples were then treated with osmium tetroxide in 0.2 M phosphate buffer for 1 h, followed by rinsing with pure water three times. The samples were subsequently dehydrated in ethanol solution at 50%, 70%, 80%, 90% and 100% three times for 10 min each. The samples were immersed in HMDS for 3 min and then stored in a desiccator overnight to avoid contamination. Finally, the dried samples were mounted on aluminium stubs and sputter coated with 10 nm of gold before SEM analysis.

2.3.2. Fourier transform infrared spectroscopy

The chitosan crosslinking was determined by using Fourier transform infrared (FTIR) spectroscopy (Varian 660-IR) with 4 cm^{-1} resolution, averaging for 32 scans. Unprocessed chitosan was analyzed as a control.

2.3.3. Equilibrium swelling ratio

The swelling behaviour of the porous hydrogel was evaluated at 37 °C, in PBS (pH 7.2–7.4) at least three times. After immersion in excessive PBS at 37 °C overnight (12 h), the swollen chitosan hydrogels were weighed (W_t). The hydrogels were subsequently lyophilized overnight, and the dry weights were recorded (W_0). The equilibrium swelling ratio (ESR) was then calculated by using the following equation:

$$\mathrm{ESR} = \frac{W_t - W_0}{W_0}.$$

2.3.4. Mechanical testing

Uniaxial compression tests were performed in an unconfined state by using a Bose ELF 3400 mechanical tester with a 50N load cell. Prior to mechanical testing, the hydrogels produced at dense gas CO_2 and atmospheric condition were swelled for 2 h in PBS. The thickness (~3 mm) and diameter (~8 mm) of each sample were measured using a digital caliper prior to mechanical testing. The compressive properties of the samples were tested in the hydrated state, at room temperature. Compression (mm) and load (N) were recorded using Wintest software at a crosshead speed of 30 μm s^{-1} and strain level of 50%. The compressive modulus was obtained as the tangent slope of the stress–strain curve.

2.3.5. Haematoxylin and eosin staining

Cell penetration and growth in the fabricated hydrogels were evaluated using light microscopy analysis on crosssections of cell-seeded hydrogels that were fixed, sectioned and stained. The cell-seeded hydrogels (at day 4 post-seeding) were fixed by soaking in 10% formalin overnight, and subsequently immersed in 70% ethanol. The fixed samples were processed on an automated tissue processor on a 6 h cycle to paraffin through a graded series of ethanol and xylene. The samples were then embedded in paraffin wax and 5 μm sections were taken and collected onto glass slides and dried. The slides were deparaffinized, rehydrated, stained using a standard haematoxylin and eosin (H&E) staining procedure, dehydrated, cleared in xylene and mounted in DPX. The samples were visualized using a light microscope (Leica) equipped with a camera.

2.3.6. Live/dead staining

Cell proliferation in the fabricated hydrogel was examined by live/dead staining. The cell-seeded hydrogels (3 h, 1, 4 and 7 days) were stained with FDA and PI (both 1 μg ml^{-1} in PBS) for 2 min. The stained samples were assessed using confocal laser scanning microscopy (CLSM, Nikon Limo). Live cells were stained fluorescent green due to intracellular esterase activity that de-acetylated FDA to a green fluorescent product. Dead cells were stained fluorescent red as their compromised membranes were permeable to nucleic acid stain (PI). Per cent cell viability values were calculated by counting the number of live (green) cells and the number of dead (red) cells on CLSM images (10 × magnification). The values were obtained by dividing the number of live cells by the number of total cells (live cells + dead cells). At least 300 cells were counted for each sample. A statistical significance level of 99.5% ($P < 0.005$) was considered in assessing the viability to avoid potential human error in cell counting.

2.3.7. In vitro proliferation assay

In vitro cell proliferation was examined by MTS assay. In brief, the cell-seeded hydrogels (1×10^4 cells $sample^{-1}$) were immersed in culture medium within individual wells of a 48-well plate dish. At different time intervals (3 h, 1, 4 and 7 days), the samples were rinsed three times with PBS; 250 μl fresh medium and 50 μl MTS was subsequently added to each well. The samples were then kept in a CO_2 (5% CO_2 and 95% humidity) incubator at 37 °C for 1 h. This allowed MTS to react with metabolically active cells and subsequently yield in water-soluble formazan product quantifiable by absorbance at 490 nm using a microplate reader (Bio Rad 680).

2.4. Statistical analysis

Statistical significance was determined for replicates of 3 ($n = 9$ for MTS assay) by an independent Student's *t*-test for two groups of data using SPSS statistical software (PASW Statistics 18). Data are represented as mean ± standard deviation (SD).

3. Results and discussion

3.1. Hydrogel fabrication under atmospheric conditions

To assess the effects of various parameters on hydrogel formation, chitosan solution was crosslinked by using two types of crosslinkers (i.e. GA and GP) at different temperatures. The results in Table 1 demonstrate that GA crosslinking was concentration, temperature and time dependent. A yellowish transparent hydrogel was formed within 1 h at 37 °C when using GA at concentrations ranging between 0.125 and 0.5 vol.%. However, no porous structure was generated on the top surface (Fig. 3a), which is undesirable for nutrient diffusion and waste exchange. At lower temperatures, e.g. 23 °C, a longer period of time was required to generate a firm hydrogel (i.e. 1.5 and 2 h, when 0.25 and 0.125 vol.% GA concentration were used, respectively). At 4 °C, a firm hydrogel was formed after 1.5 h when using 0.5 vol.% GA crosslinker; no solid hydrogel was formed after 3 h for lower GA concentrations. Longer crosslinking times were not used in this study, as these caused higher crosslinking density, which would subsequently increase the brittleness of the hydrogels, as well as decrease both swelling ratio and pore size.

GP is a naturally derived crosslinker that has been shown to be less cytotoxic and genotoxic than GA [41,42]. However, GP has less crosslinking reactivity than GA [43]. GP crosslinking showed similar concentration, temperature and time dependency as GA crosslinking. As shown in Table 1, firm hydrogels with a dark blue colour were only formed when the GP ratio was above 0.25 wt.% at 37 °C after 3 h. No porous structure was observed (as shown in Fig. 3b).

Based the results obtained, we attempted to conduct the crosslinking reaction in a dense gas system for a period of 1.5 and 3 h using GA and GP, respectively, as marked in Table 1. Preliminary tests have confirmed that shorter crosslinking times were not long

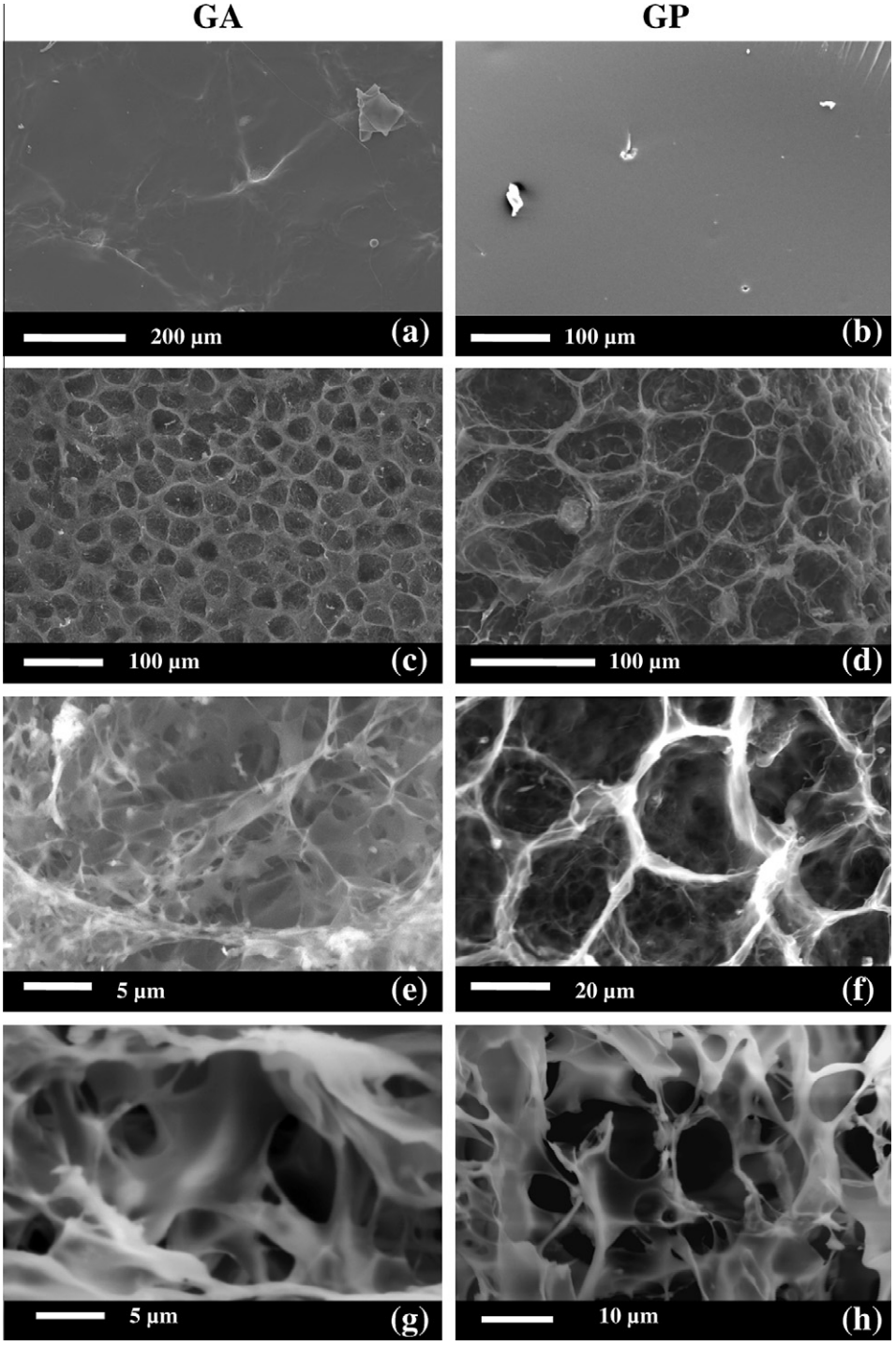

Fig. 3. SEM images of crosslinked chitosan hydrogels produced under (a and b) atmospheric conditions (P = 1 bar), and (c–h) dense gas conditions (P = 60 bar). (a, c, e, g) GA-(4 °C); (b, d, f, h) GP (37 °C). (c–f) hydrogel top surfaces; (g and h) hydrogel crosssections.

enough to create firm hydrogels under both atmospheric condition and dense gas conditions.

3.2. Hydrogel fabrication using dense gas CO_2

The feasibility of using dense gas CO_2 was assessed for the crosslinking of chitosan hydrogels with GA and GP and creation of porosity in their structure. The solubility of dense gas CO_2 in aqueous phase plays a significant role in creating porosity. The volume expansion was negligible during the pressurization stage, but in the depressurization stage, the volume expansion was more than 150%. In the presence of crosslinker, the volume expansion was reduced to 50% because the viscosity of the solution was increased. The pores are generated due to the formation of CO_2 gas phase during the depressurization process. The effects of parameters such as temperature and pressure on the properties of crosslinked chitosan hydrogels using GA and GP were demonstrated.

Porous, rigid and wet chitosan hydrogels were produced at 4 °C and 60 bar using 0.5 vol.% GA as shown in Fig. 3c, e and g; unstable hydrogels were formed at lower GA concentrations, which is

consistent with the results acquired under atmospheric conditions. At temperatures between 23 and 37 °C, transparent and non-porous hydrogels, similar to those produced under atmospheric conditions, were obtained using 60–160 bar of dense gas CO_2. The formation of non-porous structure at these temperatures may result from the rapid rate of the crosslinking reaction, which formed a skin layer on the top of the hydrogel by the Schiff base reaction [44]; this layer impeded CO_2 diffusion into the solution.

Chitosan hydrogels were fabricated at 37 °C using GP concentrations above 0.25 wt.% and CO_2 pressures between 60 and 160 bar (Fig. 3d, f and h). Higher temperatures were not used to increase the rate of crosslinking because the CO_2 solubility in aqueous solutions was decreased at these conditions, which may subsequently reduce the porosity of hydrogels. The results of our studies showed that the integrity of GA- and GP-crosslinked chitosan porous hydrogels was maintained when kept in PBS for at least 1 month.

3.3. Crosslinking characterization

FTIR spectroscopy was used to analyze the crosslinking of chitosan. Bands due to double bond stretches (1500–1800 cm^{-1}) were studied to demonstrate the chemical reaction between chitosan and crosslinkers (i.e. GA and GP). As expected, unprocessed chitosan exhibited a characteristic peak at 1588 cm^{-1}, which corresponds to amide II (N–H). Another peak was detected at 1648 cm^{-1}, corresponding to the C=O stretch for amide I, which indicated that chitosan was not completely deacetylated (Fig. 4a) [31]. GA-crosslinked hydrogels showed an obvious peak at 1700 cm^{-1} (Fig. 4b and c), which was assigned to the imine (C=N) formation [45,46]. GP-crosslinked hydrogels also exhibited a peak shift from 1640 to 1648 cm^{-1}, due to the crosslinking reaction between chitosan and GP (Fig. 4d and e) [47]. No significant difference was observed between hydrogels produced at atmospheric (1 bar) and dense gas (60 bar) conditions using GA and GP, respectively.

The crosslinking degree has been shown to be correlated to colour intensity [48,49]; the measurement of colour intensity was processed using Image J software [50]. As shown in Fig. 5, no significant difference was observed between hydrogels produced at atmospheric (1 bar) and dense gas (60 bar) conditions using GA and GP, respectively. These results indicate that the use of dense gas CO_2 had no significant effect on chitosan crosslinking. The unstable hydrogels, as shown in Table 1, was transparent and soft without noticeable mechanical integrity, and the colour intensities of these samples were much lower than those of firm hydrogels.

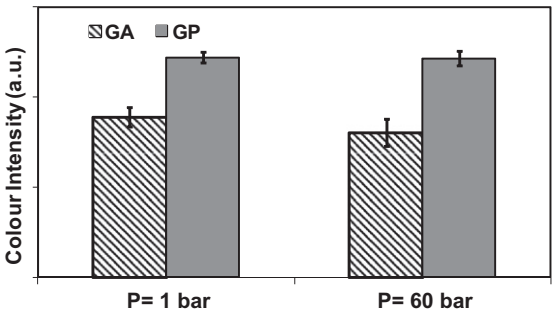

Fig. 5. Colour intensity of chitosan hydrogels measured by using Image J software ($n \geqslant 30$).

3.4. Pore characteristics

Pore size plays a critical role in tissue engineering scaffolds in terms of regulating cell behaviour and infiltration into the scaffold [36,51]. In addition, the dimensions of the pores may regulate processes such as angiogenesis in the scaffold. The formation of a non-porous skin layer is a common problem in scaffold production [52]. Skin layers block nutrient exchange and oxygen diffusion into the 3-D structure, which is undesirable for tissue engineering applications. Yannas et al. found that a collagen-based scaffold was morphologically active in an in vivo skin regeneration model, provided that the average pore diameter ranged from 20 to 125 μm on the surface [36]. In our studies, no skin layer was formed in chitosan hydrogels produced by dense gas CO_2. A porous structure was observed on both the top surface (Fig. 3c–f) and cross-section (Fig. 3g and h) of fabricated hydrogels. The average pore diameter on the surface of chitosan hydrogel fabricated using CO_2 as a pore

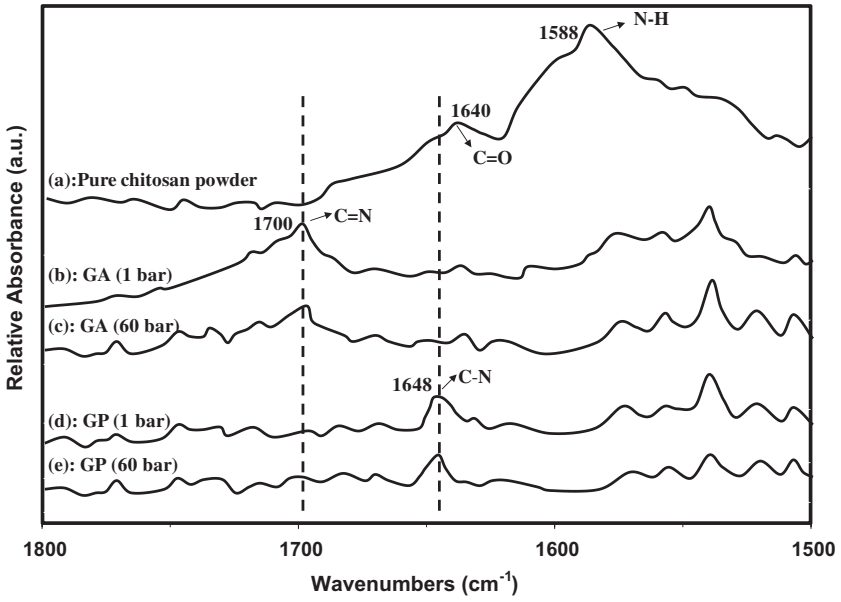

Fig. 4. (a) FTIR spectroscopy of unprocessed chitosan powder; GA-crosslinked hydrogels produced under (b) atmospheric conditions (P = 1 bar) and (c) dense gas conditions (P = 60 bar); and GP-crosslinked hydrogels at (d) 1 bar and (e) 60 bar.

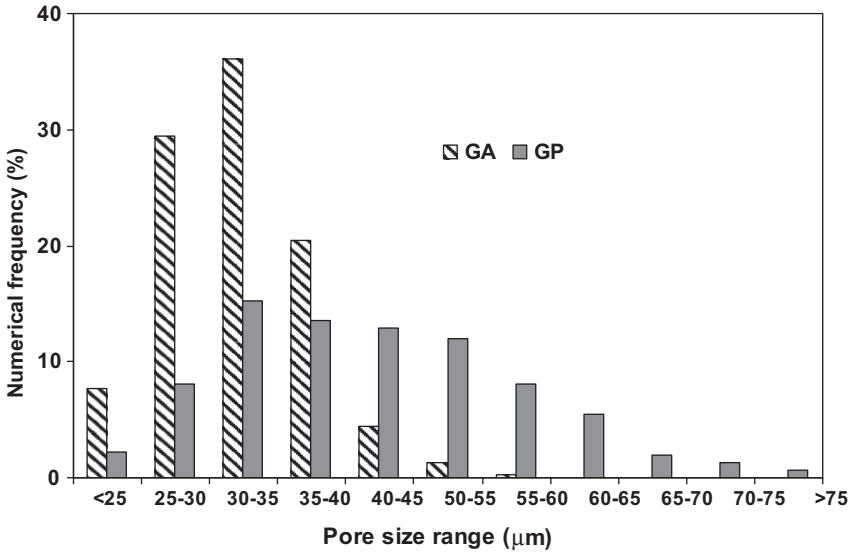

Fig. 6. Pore size distribution of GA- and GP-crosslinked chitosan hydrogels produced using dense gas CO_2.

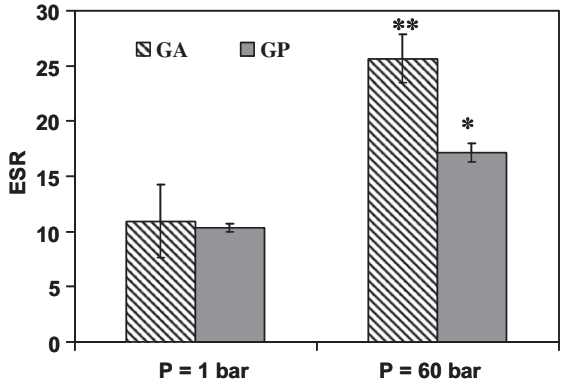

Fig. 7. The ESR of crosslinked chitosan hydrogels produced under atmospheric conditions ($P = 1$ bar) and dense gas conditions ($P = 60$ bar) using GA and GP crosslinkers. Student's t-tests were used to compare the hydrogels fabricated under dense gas conditions with those produced under atmospheric conditions: $^{*}P < 0.005$; $^{**}P < 0.0005$.

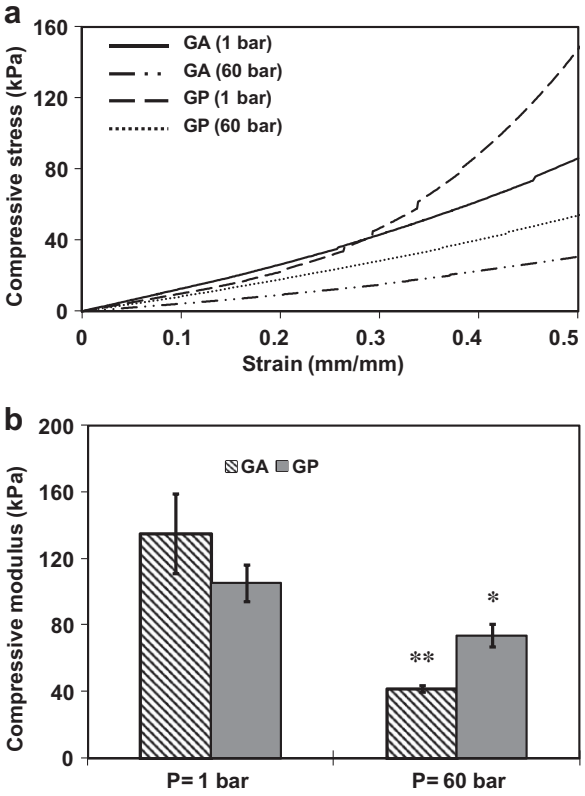

Fig. 8. (a) Compressive stress–strain curves of fabricated hydrogels; (b) compressive modulus of fabricated hydrogels under atmospheric ($P = 1$ bar) and dense gas ($P = 60$ bar) conditions. Student's t-tests were used to compare the hydrogels fabricated under dense gas conditions with those produced under atmospheric conditions $^{*}P < 0.01$; $^{**}P < 0.005$.

foaming agent at 60 bar and 4 °C was 32.0 ± 5 μm. In the GP system, the average pore diameter of these hydrogels was 43.9 ± 12 μm, which is slightly larger than those crosslinked with GA. The pore size distributions of chitosan hydrogels are shown in Fig. 6. The percentage of macropores (i.e. ⩾50 μm) in GP-crosslinked hydrogels was 30%, which is 15-fold higher than found with GA-crosslinked hydrogels (2%) (Fig. 6). The increased pore diameter and large fraction of macropores in GP-crosslinked hydrogels may be due to the difference in crosslinking density between the GA and GP systems.

Increasing the pressure had negligible effect on the pore characteristics of chitosan hydrogels produced using GA and GP. This effect can be attributed to the negligible enhancement of CO_2 solubility by elevating pressures from 60 to 160 bar. These results are consistent with a previous study of elastin-based hydrogels; the pore size of elastin hydrogels was not enhanced by increasing CO_2 pressure at 37 °C [32]. The pore diameter and orientation on the cross-section of chitosan hydrogel processed by dense gas CO_2 were similar to those on the surface. The average pore diameter of chitosan hydrogels was larger than the elastin-based gels (~5 μm) that were crosslinked with GA in aqueous system using a dense gas process [32]. This may be due to the use of a lower operating temperature (4 °C) during the crosslinking of chitosan under dense gas CO_2, which increased CO_2 solubility in aqueous phase and reduced the crosslinking rate. The pore size acquired in this study was comparable with that produced by a dense gas CO_2 templating technique [26] that involved a pre-fabricated surfactant.

A post-heating process was previously used to create open porous gelatin hydrogels [24]. Here we performed a preliminary

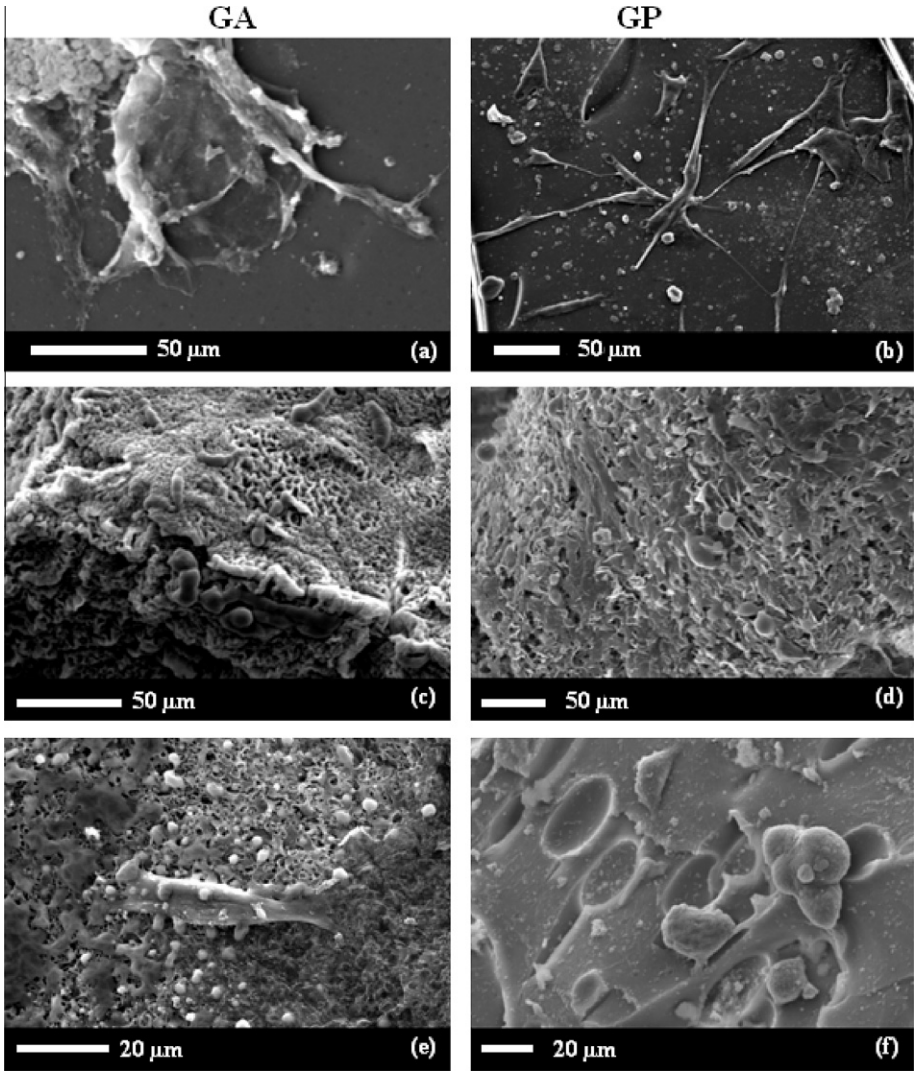

Fig. 9. SEM images of cell colonization on the surface of GA- and GP-crosslinked hydrogels produced under (a and b) atmospheric conditions, and (c–f) dense gas conditions. (a–d) hydrogel top surfaces; (e and f) hydrogel crosssections.

investigation to determine the effect of post-heating (70 °C and 10 min) on the pore characteristics of hydrogels fabricated from chitosan. The SEM results showed that the pore characteristics of chitosan hydrogel were not changed significantly after this treatment. This result is consistent with previous data obtained for chitin [29].

The porous 3-D chitosan hydrogel produced in this study has potential applications in neovascularization, and cellular ingrowth [17,53]. Further characterizations such as swelling and mechanical behaviours and in vitro cell culture tests were carried out on chitosan crosslinked with 0.5 vol.% GA for a period of 1.5 h at 4 °C under both atmospheric conditions and 60 bar CO_2 pressure. Chitosan samples were also produced using 0.25 wt.% GP crosslinker for a period of 3 h at 37 °C and 60 bar.

3.5. Equilibrium swelling ratio

The rate of diffusion of nutrient and exchange of waste in hydrogel scaffolds depends on the swelling behaviour of hydrogel. In general, crosslinked chitosan hydrogel under dense gas CO_2 conditions exhibited higher ESRs than the samples produced under atmospheric conditions (Fig. 7). This effect was more noticeable when using GA crosslinker: the ESR of GA-crosslinked hydrogels produced with dense gas was 25.7 ± 2.2, which is more than 2-fold higher than the samples produced under atmospheric conditions (10.9 ± 3.3). The lower swelling ratio of the latter samples resulted from the absence of porous structure. A similar pattern was observed in the GP-crosslinked hydrogel system. GP-crosslinked hydrogels produced under dense gas conditions displayed an ESR of 17.2 ± 0.8, while under atmospheric conditions the ESR was decreased to 10.3 ± 0.4. The swelling properties of chitosan hydrogels processed in dense gas CO_2 at 37 °C in PBS was comparable with the ones produced by other methods for various tissue engineering applications [8,54–58].

3.6. Mechanical characterizations

Adequate mechanical strength is desirable for hydrogels in tissue engineering. The compressive moduli of hydrogels depend on the nature of materials, degree of crosslinking and pore size. It is not feasible to compare the mechanical properties of hydrogels produced using GA and GP, because operating parameters such as crosslinking agents, temperature and processing time were different in both systems. Therefore, comparison was only made between the hydrogels produced at different pressures (1 and 60 bar) for each crosslinker. The compressive properties of

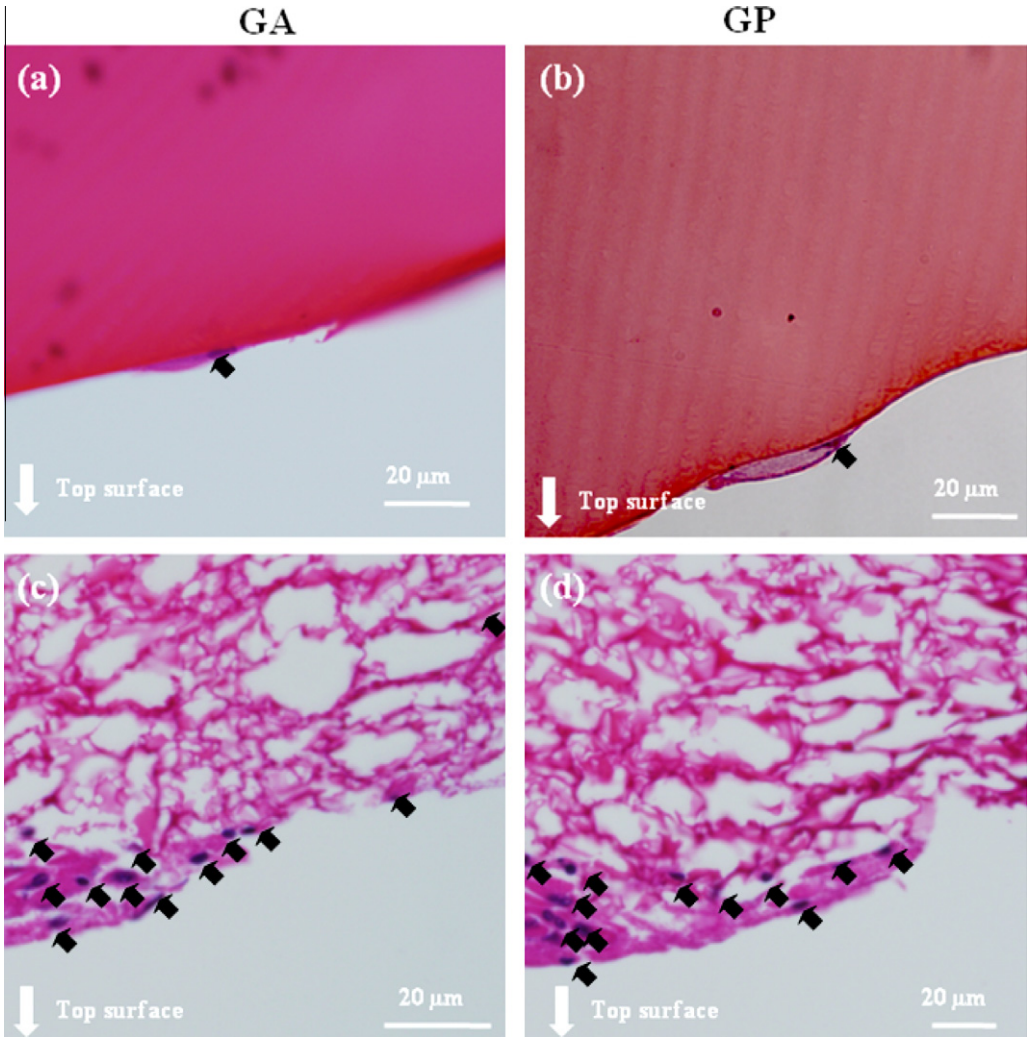

Fig. 10. Light microscopy images of cell-seeded chitosan hydrogels produced under (a and b) atmospheric conditions, and (c and d) dense gas conditions. (a and c) GA; (b and d) GP. Black arrows indicate the positions of cells.

GA- and GP-crosslinked chitosan hydrogels produced under atmospheric conditions and using dense gas CO_2 are shown in Fig. 8A. The stress–strain curve becomes non-linear at 20–30% strain for both GA- and GP-crosslinked hydrogels produced under atmospheric conditions. This indicates that plastic deformation occurred in the hydrogel produced under atmospheric conditions at strains greater than 30%. There is no significant difference in the mechanical properties of hydrogels produced by GA and GP at 1 bar. Hydrogels produced by using dense gas CO_2 as a pore foaming agent exhibited an almost linear stress–strain curve at 50% strain. The results demonstrate that hydrogels produced using dense gas conditions were expected to be more elastic than those produced under atmospheric conditions. The compressive modulus of GA- and GP-crosslinked hydrogels produced using dense gas conditions was lower (41.6 ± 2 and 73.9 ± 7 kPa, respectively) than those produced under atmospheric condition (135.1 ± 24 and 105.2 ± 11 kPa, respectively) (Fig. 8B). The decrease in modulus was due to the increased porosity of chitosan produced by dense gas CO_2. Chitosan hydrogels produced using dense gas CO_2 exhibited higher compressive modulus than elastin (1.9 ± 0.1 kPa) and elastin/tropoelastin (4.9–11.8 kPa) composite hydrogels fabricated using dense gas CO_2 in an aqueous-based system [59], which is due to the nature of biopolymer used. The compressive behaviours of fabricated hydrogels have been reported to be correlated with the swelling properties [32]. In our study, GA-crosslinked hydrogels exhibited higher ESR, but lower compressive moduli, than GP-system. This phenomenon is consistent with the data previously published by Srokowski et al. where lower swelling ratio for lysine diisocyanate-crosslinked hydrogels exhibited higher compressive modulus [60].

3.7. In vitro cell proliferation

One of the important properties of hydrogel is to support cellular growth and proliferation in 3-D structures. The feasibility of using fabricated chitosan hydrogels for tissue engineering applications was assessed by using various analytical techniques including SEM, histological study, live/dead staining and MTS assay on the cell-seeded hydrogels.

SEM images indicated that cells were able to attach and grow on the top surface of both GA- and GP-crosslinked hydrogels fabricated under atmospheric conditions and using dense gas CO_2 (Fig. 9). The hydrogels fabricated under atmospheric conditions only allow for cell attachment and colonization on the surface as depicted in Fig. 9a and b with no cellular penetration into 3-D structures. However, fibroblasts were able to adhere on the top surface of fabricated hydrogels (Fig. 9c and d) and also penetrate into the 3-D structure of hydrogels (Fig. 9e and f) fabricated using dense gas CO_2. This effect was due to the presence of porous struc-

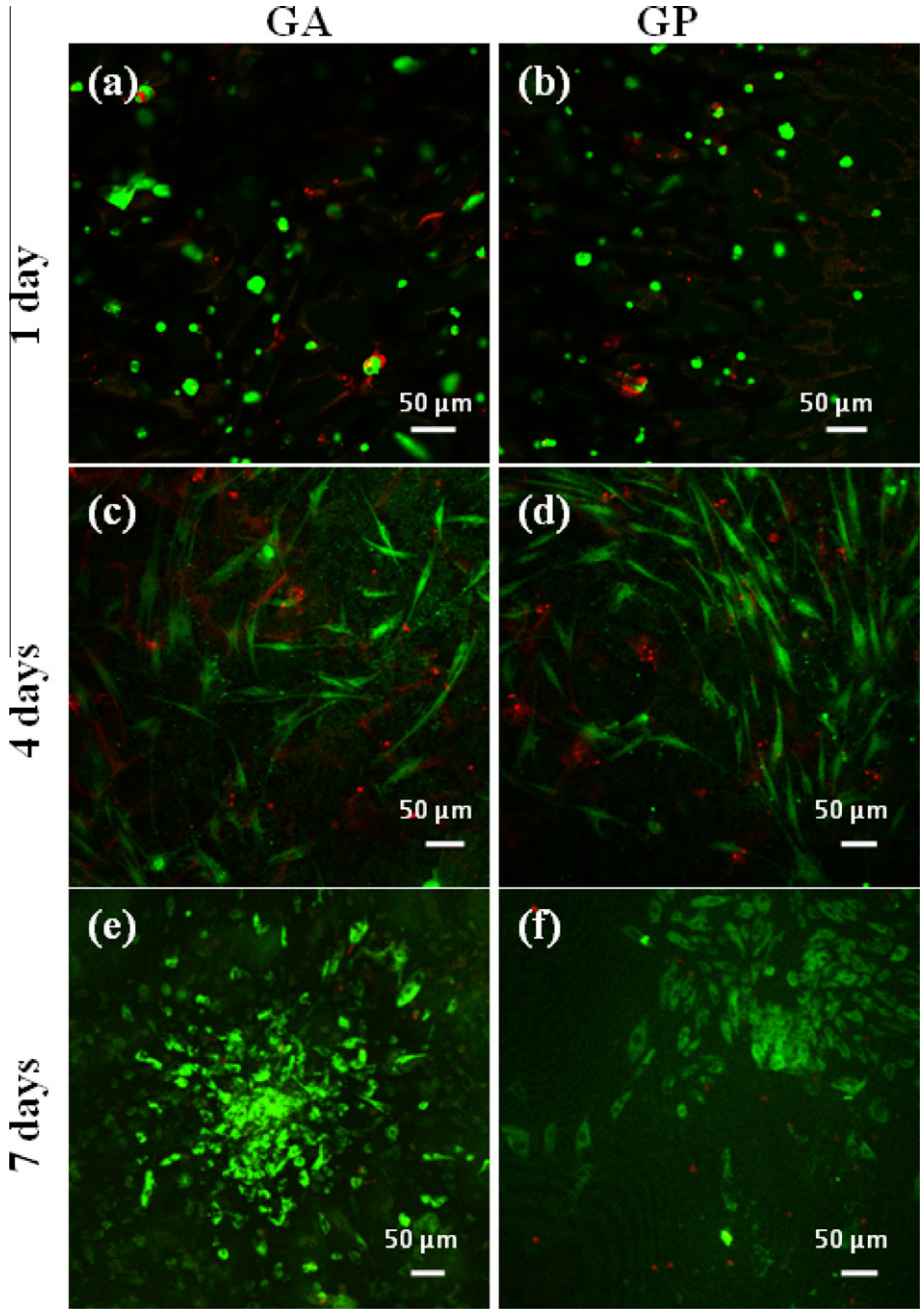

Fig. 11. CLSM images of cell-seeded chitosan hydrogels produced under dense gas conditions after (a and b) 1 day, (c and d) 4 days and (e and f) 7 days post-seeding. (a, c, e) GA-crosslinked hydrogels. (b, d, f) GP-crosslinked hydrogels.

ture on the top surface, which can swell in an aqueous media, allowing cell infiltration.

The cell penetration was further determined by histological analysis after H&E staining. As shown in Fig. 10a and b, both GA- and GP-crosslinked hydrogels produced under atmospheric conditions exhibited non-porous structure, and cells could only attach on the top surface. These results are consistent with SEM images. However, cells were able to penetrate into the 3-D structure of the fabricated hydrogels produced using dense gas CO_2 due to the presence of a porous structure as depicted in Fig. 10c and d. Cell penetration is a function of surface morphology, pore interconnectivity and oxygen diffusion; a maximum penetration of 150–200 μm into porous scaffolds without vascular structure formation has been reported [61]. As shown in Fig. 10c and d, fibroblast cell proliferation into the 3-D structure of chitosan hydrogel fabricated by the dense gas process was considerably improved due to the presence of porosity in the 3-D structure. The low cell density may be due to oxygen availability and the small fraction of pores with sizes above 50 μm. Cellular penetration can be enhanced by increasing the pore size of chitosan hydrogels. This can be achieved by increasing the solubility of CO_2 in aqueous phase, which will result in the formation of large pores.

Cell proliferation on the hydrogels produced by dense gas CO_2 was assessed using CLSM images as shown in Fig. 11. Cells were maintained as spherical shapes after 1 day of cell-seeding on both GA- and GP-crosslinked hydrogels as indicated in Fig. 11a and b. After 4 days of culture, cells became spindle-shaped, indicating that cells attached and grew on the hydrogels (Fig. 11c and d). The number of live cells was increased dramatically at day 7 (Fig. 11e and f), which showed cell proliferation on the fabricated

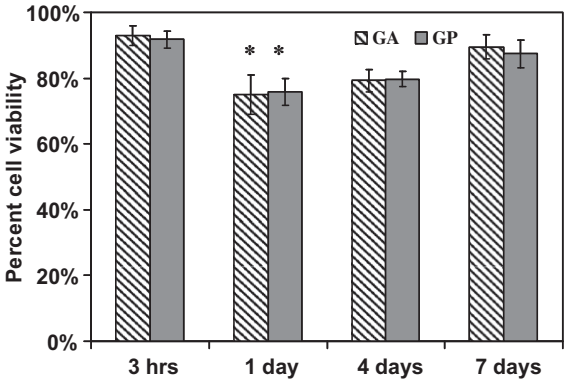

Fig. 12. Viability of cell-seeded GA- and GP-crosslinked hydrogels under dense gas conditions and at different times post-seeding. Student's *t*-tests were performed for all samples compared with samples at 3 h: $^{*}P < 0.005$.

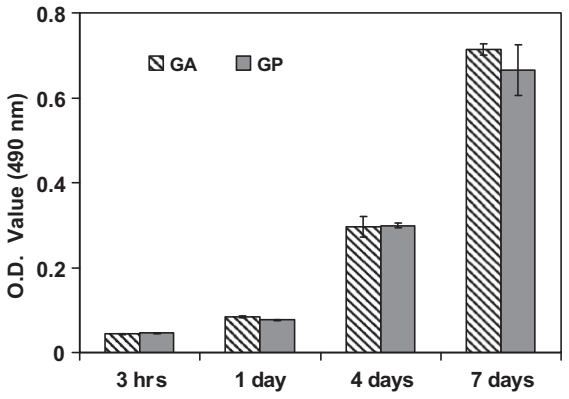

Fig. 13. MTS analysis on GA- and GP-crosslinked chitosan hydrogels fabricated using dense gas conditions at different times post-seeding ($n = 9$).

hydrogels. The degree of cell viability was assessed by cell counting. The fraction of viable cells seeded on GA- and GP-crosslinked chitosan hydrogels obtained from live/dead cell counting based on CLSM images are shown in Fig. 12. GA-crosslinked hydrogels demonstrated an initial cell viability of ~93% (3 h after cell seeding). A statistically significant drop in viability was observed after 1 day of in vitro culture (75%). This can be explained by cell death due to manipulation and lack of proliferation during the early stages of culture. The cell viability was increased to 79% at day 4, and it continued to increase, approaching 89% at day 7. No significant difference (99.5% confidence level) was observed between day 7 and the initial condition (3 h). GP-crosslinked hydrogels exhibited a similar pattern of cell viability. MTS analysis also confirmed cellular proliferation on fabricated constructs using dense gas CO_2; as shown in Fig. 13, the optical density (OD) at 490 nm increased with culture time for both GA- and GP-crosslinked hydrogels. Significant increases in OD value were observed at days 4 and 7, indicating that cell proliferation commenced from day 4 and continued to day 7. These results are consistent with cell viability data obtained from live/dead staining. The results of in vitro studies demonstrate that porous chitosan hydrogel fabricated using dense gas CO_2 is a suitable candidate for cell proliferation and growth.

4. Conclusion

Dense gas CO_2 was efficient as a pore forming agent for creating 3-D biopolymer hydrogels that are both homogenous and porous. The average pore size in the chitosan system ranged from 30 to 40 μm using GA and GP as crosslinker, respectively. This process is rapid compared with using freeze-drying, eliminates skin layer formation on the surface of hydrogels scaffolds, and minimizes the use of organic solvents and surfactants. In vitro cell culturing tests showed that the fabricated hydrogels were able to support cellular penetration and proliferation within the 3-D structure, suggesting that these are promising materials for tissue engineering applications. Different strategies will be used in future study to enhance the distance of cellular penetration; these methods include increasing CO_2 solubility in the aqueous phase and the creation of macroarchitecture in chitosan hydrogel.

Acknowledgement

The authors acknowledge the financial support of ARC Grant No. DP0988545.

Appendix A. Figures with essential colour discrimination

Certain figures in this article, particularly Figs. 1, 10, and 11 are difficult to interpret in black and white. The full colour images can be found in the on-line version, at doi:10.1016/j.actbio.2010.11.043.

References

[1] Burg KJL, Holder Jr WD, Culberson CR, Beiler RJ, Greene KG, Loebsack AB, et al. Comparative study of seeding methods for three-dimensional polymeric scaffolds. J Biomed Mater Res 2000;51:642–9.
[2] Ma PX. Biomimetic materials for tissue engineering. Adv Drug Deliv Rev 2008;60:184–98.
[3] VandeVord PJ, Matthew HWT, DeSilva SP, Mayton L, Wu B, Wooley PH. Evaluation of the biocompatibility of a chitosan scaffold in mice. J Biomed Mater Res 2002;59:585–90.
[4] Peppas N, Hilt JZ, Khademhosseini A, Langer R. Hydrogels in biology and medicine. Adv Mater 2006;18:1–17.
[5] Verheul RJ, Amidi M, van Steenbergen MJ, van Riet E, Jiskoot W, Hennink WE. Influence of the degree of acetylation on the enzymatic degradation and *in vitro* biological properties of trimethylated chitosans. Biomaterials 2009;30:3129–35.
[6] Suh JK, Matthew HW. Application of chitosan-based polysaccharide biomaterials in cartilage tissue engineering: a review. Biomaterials 2000;21:2589–98.
[7] Lee KY, Ha WS, Park WH. Blood compatibility and biodegradability of partially N-acylated chitosan derivatives. Biomaterials 1995;16:1211–6.
[8] Ma L, Gao C, Mao Z, Zhou J, Shen J, Hu X, et al. Collagen/chitosan porous scaffolds with improved biostability for skin tissue engineering. Biomaterials 2003;24:4833–41.
[9] Shanmugasundaram N, Ravichandran P, Neelakanta Reddy P, Ramamurty N, Pal S, Panduranga Rao K. Collagen-chitosan polymeric scaffolds for the in vitro culture of human epidermoid carcinoma cells. Biomaterials 2001;22:1943–51.
[10] Mwale F, Iordanova M, Demers CN, Steffen T, Roughley P, Antoniou J. Biological evaluation of chitosan salts cross-linked to genipin as a cell scaffold for disk tissue engineering. Tissue Eng 2005;11:130–40.
[11] Lu G, Kong L, Sheng B, Wang G, Gong Y, Zhang X. Degradation of covalently cross-linked carboxymethyl chitosan and its potential application for peripheral nerve regeneration. Eur Polym J 2007;43:3807–18.
[12] Hsieh C-Y, Tsai S-P, Ho M-H, Wang D-M, Liu C-E, Hsieh C-H, et al. Analysis of freeze-gelation and cross-linking processes for preparing porous chitosan scaffolds. Carbohydr Polym 2007;67:124–32.
[13] Wan Y, Wu H, Cao X, Dalai S. Compressive mechanical properties and biodegradability of porous poly(caprolactone)/chitosan scaffolds. Polym Degrad Stab 2008;93:1736–41.
[14] Wu H, Wan Y, Cao X, Wu Q. Proliferation of chondrocytes on porous poly(DL-lactide)/chitosan scaffolds. Acta Biomater 2008;4:76–87.
[15] Madihally SV, Matthew HWT. Porous chitosan scaffolds for tissue engineering. Biomaterials 1999;20:1133–42.
[16] Hsieh WC, Chang CP, Lin SM. Morphology and characterization of 3D micro-porous structured chitosan scaffolds for tissue engineering. Colloids Surf B 2007;57:250–5.
[17] Annabi N, Nichol JW, Zhong X, Ji C, Koshy S, Khademhosseini A, et al. Controlling the porosity and microarchitecture of hydrogels for tissue engineering. Tissue Eng Part B 2010;16:371–83.
[18] Davies OR, Lewis AL, Whitaker MJ, Tai H, Shakesheff KM, Howdle SM. Applications of supercritical CO_2 in the fabrication of polymer systems for drug delivery and tissue engineering. Adv Drug Deliv Rev 2008;60:373–87.

[19] Pini R, Storti G, Mazzotti M, Tai H, Shakesheff KM, Howdle SM. Sorption and swelling of poly(DL-lactic acid) and poly(lactic-co-glycolic acid) in supercritical CO_2: an experimental and modeling study. J Polym Sci, Part B: Polym Phys 2007;46:483–96.
[20] Mathieu LM, Mueller TL, Bourban P-E, Pioletti DP, Mueller R, Manson J-AE. Architecture and properties of anisotropic polymer composite scaffolds for bone tissue engineering. Biomaterials 2006;27:905–16.
[21] Singh L, Kumar V, Ratner BD. Generation of porous microcellular 85/15 poly (DL-lactide-co-glycolide) foams for biomedical applications. Biomaterials 2004;25:2611–7.
[22] Tai H, Mather ML, Howard D, Wang W, White LJ, Crowe JA, et al. Control of pore size and structure of tissue engineering scaffolds produced by supercritical fluid processing. Eur Cells Mater 2007;14:64–77.
[23] Mooney DJ, Baldwin DF, Suh NP, Vacanti JP, Langer R. Novel approach to fabricate porous sponges of poly(D,L-lactic-co-glycolic acid) without the use of organic solvents. Biomaterials 1996;17:1417–22.
[24] Shih HH, Lee KR, Lai HM, Tsai CC, Chang YC. Method of making porous biodegradable polymers. US 66732862003.
[25] Partap S, Rehman I, Jones JR, Darr JA. Supercritical carbon dioxide in water emulsion-templated synthesis of porous calcium alginate hydrogels. Adv Mater 2006;18:501–4.
[26] Lee JY, Tan B, Cooper AI. CO_2-in-water emulsion-templated poly(vinyl alcohol) hydrogels using poly(vinyl acetate)-based surfactants. Macromolecules 2007;40:1955–61.
[27] Bing Z, Lee JY, Choi SW, Kim JH. Preparation of porous $CaCO_3$/PAM composites by CO_2 in water emulsion templating method. Eur Polym J 2007;43:4814–20.
[28] Temtem M, Silva LMC, Andrade PZ, dos Santos F, da Silva CL, Cabral JMS, et al. J Supercrit Fluids 2009;48:269.
[29] Tsioptsias C, Panayiotou C. Foaming of chitin hydrogels processed by supercritical carbon dioxide. J Supercrit Fluid 2008;47:302–8.
[30] Singh J, Dutta PK, Dutta J, Hunt AJ, Macquarrie DJ, Clark JH. Preparation and properties of highly soluble chitosan-L-glutamic acid aerogel derivative. Carbohydr Polym 2009;76:188–95.
[31] Ji C, Barrett A, Poole-Warren Laura A, Foster NR, Dehghani F. The development of a dense gas solvent exchange process for the impregnation of pharmaceuticals into porous chitosan. Int J Pharm 2010;391:187–96.
[32] Annabi N, Mithieux SM, Weiss AS, Dehghani F. The fabrication of elastin-based hydrogels using high pressure CO_2. Biomaterials 2009;30:1–8.
[33] Dodds WS, Stutzman LF, Sollami BJ. Carbon dioxide solubility in water. Ind Eng Chem 1956;1:92.
[34] Dehghani F, Annabi N, Valtchev P, Mithieux SM, Weiss AS, Kazarian SG, et al. Effect of dense gas CO_2 on the coacervation of elastin. Biomacromolecules 2008;9:1100–5.
[35] Jayakrishnan A, Jameela SR. Glutaraldehyde as a fixative in bioprostheses and drug delivery matrices. Biomaterials 1996;17:471.
[36] Yannas IV, Lee E, Orgill DP, Skrabut EM, Murphy GF. Synthesis and characterization of a model extracellular matrix that induces partial regeneration of adult mammalian skin. Proc Natl Acad Sci USA 1989;86:933–7.
[37] Ginty PJ, Howard D, Upton CE, Barry JJA, Rose FRAJ, Shakesheff KM, et al. A supercritical CO_2 injection system for the production of polymer/mammalian cell composites. J Supercrit Fluids 2008;43:535–41.
[38] Dillow AK, Dehghani F, Hrkach JS, Foster NR, Langer R. Bacterial inactivation by using near- and supercritical carbon dioxide. Proc Natl Acad Sci USA 1999;96:10344–8.
[39] Ellis JL, Titone JC, Tomasko DL, Annabi N, Dehghani F. Supercritical CO_2 sterilization of ultra-high molecular weight polyethylene. J Supercrit Fluids 2010;52:235–40.
[40] Romeo T. A simple cold-block procedure for the SEM. Aust Electron Microsc Newslett 1996;52:16–8.
[41] Tsai CC, Huang RN, Sung HW, Liang HC. *In vitro* evaluation of the genotoxicity of a naturally occurring crosslinking agent (genipin) for biologic tissue fixation. J Biomed Mater Res 2000;52:58.
[42] Chen YS, Chang JY, Cheng CY, Tsai FJ, Yao CH, Liu BS. An *in vivo* evaluation of a biodegradable genipin-cross linked gelatin peripheral nerve guide conduit material. Biomaterials 2005;26:18.
[43] Chen SC, Wu YC, Mi F-L, Lin YH, Yu LC, Sung HW. A novel pH-sensitive hydrogel composed of N,O-carboxymethyl chitosan and alginate cross-linked by genipin for protein drug delivery. J Control Release 2004;96:285.
[44] Yu H, Lu J, Xiao C. Preparation and properties of novel hydrogels form oxidized konjac glucomannan cross-linked chitosan for *in vitro* drug delivery. Macromol Biosci 2007;7:1100.
[45] Chalmers JM, Dent G. Industrial analysis with vibrational spectroscopy. Cambridge: Royal Society of Chemistry; 1997.
[46] Wang T, Turan M, Gunasekaran S. Selected properties of pH-sensitive, biodegradable chitosan–poly(vinyl alcohol) hydrogel. Polym Int 2004;53:911–8.
[47] Mi FL. Synthesis and characterization of a novel chitosan−gelatin bioconjugate with fluorescence emission. Biomacromolecules 2005;6:975–87.
[48] Chen H, Ouyang W, Lawuyi B, Martoni C, Prakash S. Reaction of chitosan with genipin and its fluorogenic attributes for potential microcasule membrane characterization. J Biomed Mater Res A 2005;75:917–27.
[49] Huang RYM, Pal R, Moon GY. Crosslinked chitosan composite membrane for the pervaporation dehydration of alcohol mixtures and enhancement of structural stability of chitosan/polysulfone composite membranes. J Membr Sci 1999;160:17–30.
[50] Annabi N, Fathi A, Mithieux SM, Martens P, Weiss AS, Dehghani F. The effect of elastin on chondrocyte adhesion and proliferation on poly(ε-caprolactone)/elastin composites. Biomaterials 2010, in press.
[51] Berry CC, Campbell G, Spadiccino A, Robertson M, Curtis ASG. The Influence of microscale topography on fibroblast attachment and motility. Biomaterials 2004;25:5781.
[52] Goel SK, Beckman EJ. Generation of microcellular polymeric foams using supercritical carbon dioxide. II: cell growth and skin formation. Polym Eng Sci 1994;34:1148–56.
[53] Whang K, Healy KE, Elenz DR, Nam EK, Tsai DC, Thomas CH, et al. Engineering bone regeneration with bioabsorbable scaffolds with novel microarchitecture. Tissue Eng 1999;5:35.
[54] Chen KY, Liao WJ, Kou SM, Tsai FJ, Chen YS, Huang CY, et al. Asymmetric chitosan membrane containing collagen. I. Nanospheres for skin tissue engineering. Biomacromolecules 2009;10:1642–9.
[55] Kathuria N, Tripathi A, Kar KK, Kumar A. Synthesis and characterization of elastic and macroporous chitosan–gelatin cryogels for tissue engineering. Acta Biomater 2009;5:406–18.
[56] Shang J, Shao ZZ, Chen X. Chitosan-based electroactive hydrogel. Polymer 2008;49:5520–5.
[57] Silva SS, Motta A, Rodrigues MT, Pinheiro AFM, Gomes ME, Mano JF, et al. Genipin-cross-linked chitosan silk fibroin sponges for cartilage engineering strategies. Biomacromolecules 2008;9:2764–74.
[58] Tan H, Chu Constance R, Payne KA, Marra Kacey G. Injectable *in situ* forming biodegradable chitosan-hyaluronic acid based hydrogels for cartilage tissue engineering. Biomaterials 2009;30:2499–506.
[59] Annabi N, Mithieux SM, Weiss AS, Dehghani F. Cross-linked open-pore elastic hydrogels based on tropoelastin, elastin and high pressure CO_2. Biomaterials 2010;31:1655–65.
[60] Srokowski EM, Woodhouse KA. Development and characterisation of novel cros-linked bio-elastomeric materials. J Biomater Sci Polym Ed 2008;19:785–99.
[61] Annabi N, Mithieux SM, Boughton EA, Ruys AJ, Weiss AS, Dehghani F. Synthesis of highly porous crosslinked elastin hydrogels and their interaction with fibroblasts *in vitro*. Biomaterials 2009;30:4550–7.